


RESEARCH

Open Access

Individualized body bioelectrical impedance parameters in newly diagnosed cancer children



Taira Teresa Batista Luna^{1,2,3}, Maraelys Morales González³, Manuel Verdecia Jarque⁴, Tamara Rubio González⁵, Soraida Candida Acosta Brooks⁶, Antonio Rafael Selva Castañeda⁷, Justa Carmen Columbié Regüíferos⁸, Victoriano Gustavo Sierra González⁹ and Luis Enrique Bergues Cabrales^{10*} 

Abstract

Background: The bioelectric impedance analysis permits to estimate electrical parameters and body composition of subjects who are either apparently healthy or sick with different pathologies. The aim of this study is to individualize the analysis of body bioelectrical impedance parameters in newly diagnosed cancer children, by means of the bioelectrical impedance analysis for each age group, gender and cancer histological variety.

Methods: This retrospective cross-sectional study consisted of 43 pediatric patients with different histological varieties of cancer, ages from 2 to 17. The body electrical resistance and body capacitive electrical reactance were measured with the Bodystat 1500-MDD analyzer. From these two electrical parameters the body electrical impedance modulus and the body phase angle were calculated.

Results: The results showed that 93.02% of cancer children were outside reference rectangles according to age groups and gender were showed. The values of body capacitive electrical reactance (72.5%) and body phase angle (90.70%) of these patients were below the lower limits of their respective rectangles. These findings were noticeable for patients who had solid tumors.

Conclusions: The BIA is feasible to individualize body bioelectrical parameters and body bioelectric state in newly diagnosed cancer children and how differ from those in apparently healthy subjects, for the same age group and gender. Additionally, the tumor electrical properties may have a noticeable role in changes of body bioelectric-physiological parameters of these newly diagnosed cancer children.

Keywords: Bodystat 1500-MDD analyzer, Body electrical resistance, Body capacitive electrical reactance, Body phase angle, Bioelectrical impedance analysis, Newly diagnosed cancer children

* Correspondence: berguesc@yahoo.com

¹⁰Departamento de Investigaciones, Centro Nacional de Electromagnetismo Aplicado, Universidad de Oriente, Ave. Las Américas s/n, 90400 Santiago de Cuba, Cuba

Full list of author information is available at the end of the article



© The Author(s). 2020 **Open Access** This article is licensed under a Creative Commons Attribution 4.0 International License, which permits use, sharing, adaptation, distribution and reproduction in any medium or format, as long as you give appropriate credit to the original author(s) and the source, provide a link to the Creative Commons licence, and indicate if changes were made. The images or other third party material in this article are included in the article's Creative Commons licence, unless indicated otherwise in a credit line to the material. If material is not included in the article's Creative Commons licence and your intended use is not permitted by statutory regulation or exceeds the permitted use, you will need to obtain permission directly from the copyright holder. To view a copy of this licence, visit <http://creativecommons.org/licenses/by/4.0/>.

Highlights

- Body bioelectrical impedance parameters in newly diagnosed cancer children.
- Body electrical capacity of the patient and net electrical capacity of the tumor in newly diagnosed cancer children.
- Total electrical capacity of the healthy tissue and overall electrical capacity of the surrounding healthy tissue-tumor interface in newly diagnosed cancer children.
- Rectangular tolerance regions.

Background

The malignant tumor is the second cause of morbidity and mortality in Cuba and worldwide. The number of cancer patients is expected to increase progressively in the next years [1]. In Cuba, cancer is the first cause of death for patients ages 5 to 15 and the second cause of death in children between 1 and 4 years old [2]. These statistics are similar to those reported in other countries [1]. Around 400 children are diagnosed each year in Cuba and 35 of them correspond approximately to Santiago de Cuba province. This number has increased to 60 in the last triennium [2]. Acute lymphoblastic leukemia, central nervous system tumors, lymphomas, bone tumors and renal tumors are the most common malignant neoplasms in pediatric patients (1–18 years old) [2–4].

Cancer in pediatric patients can be diagnosed by clinical method and laboratory, pathologic and imaging tests [5]. Additionally, electrical impedance tomography, diffusion tensor magnetic resonance imaging, magnetic resonance electrical impedance tomography, magnetic induction tomography, magnetoacoustic tomography, Hall effect imaging and magnetoacoustic tomography with magnetic induction techniques have been suggested to electrically differentiate cancer from its surrounding healthy tissue based on differences between their electrical properties [6]. Tissue electrical properties have also been used to estimate the body composition, body water, among others in subjects who are either apparently healthy or sick with different pathologies by means of the bioelectric impedance analysis (BIA) [7, 8].

The BIA permits the estimation of different body bioelectric parameters, such as the body electrical resistance (R), body capacitive electrical reactance (Xc), body electrical impedance modulus ($|Z|$) and body phase angle (θ). Parameters R and Xc have been related to the body hydration status and body cell mass of subjects who are either apparently healthy or sick with different pathologies. These relationships have been established by means of different estimation equations [9–12]. The parameter θ is associated with the pathology severity and the quality of life, survival and prognosis of the evolution of a patient [8, 13–15]. In addition, BIA has been used to

establish the normal intervals (means \pm standard deviations) of R, R/H, Xc, Xc/H and θ of different populations of apparently healthy subjects in different countries [16, 17]. The variables H, R/H and Xc/H are the height of the subject, the body electrical resistance per unit of height and the body capacitive electrical reactance per unit of height, respectively.

Normal intervals of R/H, Xc/H and θ for a population of apparently healthy subjects of Santiago de Cuba, Cuba, by gender and age groups (2–80) are reported in [16]. For this, the BioScan 98 BIA analyzer (Biológica Tecnología Médica SL, Barcelona, Spain, available at <http://www.biologico.es>) is used. In addition, the Bland-Altman statistical method is used to assess the agreement between the BioScan 98 BIA analyzer and the Bodystat 1500-MDD BIA analyzer (Bodystat Firm Inc., Tampa, Florida, USA, available at <http://www.bodystat.com>) [18], as suggested in other studies [19, 20]. Values of R, Xc and θ generated with two devices are equals when correction factors for R and Xc are introduced in the BioScan 98 (+ 14.7 Ω for R and + 22 Ω for Xc) and Bodystat 1500 MDD (– 3 Ω for R and + 9 Ω for Xc) BIA analyzers, as demonstrated in [18]. Consequently, these two BIA analyzers may be suitable in clinics. When the corrected and uncorrected R and Xc values are entered in any of total body water estimation equations, non-significant differences are reported from the statistical and clinical points of view [21]. This finding has been also observed for the fat free mass when the corrected and uncorrected R and Xc values are introduced in each one their estimation equations [22]. In these two studies, both BioScan 98 and Bodystat 1500-MDD BIA analyzers are used to estimate these values of R and Xc.

It is well documented in the literature that the bivariate analysis is one of the simplest forms of statistical analysis. It consists of the relationships between pairs of variables in a data set. This bivariate analysis usually involves the variables X and Y [23, 24]. Bivariate statistics has been extended to different problems of the science [25], specifically in the area of the bioelectrical impedance, known as the bioelectrical impedance vector analysis (BIVA). Piccoli is a pioneer of BIVA method [8, 26–28].

In BIVA plot, the variables X and Y are R/H (R) and Xc/H (Xc), respectively. Additionally, the reference intervals for any individual are represented in BIVA plots as 50, 75 and 95% tolerance ellipses obtained from apparently healthy population [8, 28]. This idea has been extended to other BIA studies [16, 29, 30].

BIVA method is valid if the variables R/H and Xc/H (R and Xc) are highly correlated, as reported in previous studies [8, 23, 26–29]. In medicine, correlation strength has been classified in perfect ($r^* = 1.0$), very strong ($0.8 < r^* < 0.9$), moderate ($0.6 < r^* < 0.7$), fair ($0.3 < r^* < 0.5$), poor ($0.1 < r^* < 0.2$) and none ($r^* = 0.0$), where r^* is the correlation coefficient of Pearson [31].

Although BIA has been used in pediatric patients with cancer [14, 32–35], we are not aware of its use to differentiate bioelectric parameters of newly diagnosed cancer children or untreated cancer children with those of apparently healthy population, by gender, age group and cancer type. The aim of this study is to individualize the analysis of body bioelectrical impedance parameters in newly diagnosed cancer children, by means of the bioelectrical impedance analysis for each age group, gender and cancer histological variety. Values of R/H , X_c/H and θ of patients with solid tumor (Ts) and non-solid tumor (Tns) are compared with those estimated in apparently healthy pediatric subjects reported in [16].

Methods

General characteristics of the research

The retrospective clinical research was cross-sectional and carried out in the Oncology and Hematology department of the hospital Infantil Sur Antonio María Béguez César, Santiago de Cuba, Cuba. The research period lasted one year (7 September 2009–10 September 2010).

Ethical considerations

This retrospective clinical research was ruled by the ethical standards of the World Medical Association Declaration of Helsinki [36]. It was authorized by the Oncology and Hematology department and approved by the Ethics Committee (Current Controlled trials BIANCANCER12032009, 12 March 2009) and Scientific Board of the hospital Infantil Sur Antonio María Béguez César, Santiago de Cuba. This trial registry was conserved in the Teaching Vice-direction of this hospital. The date of enrolment of the first participant to the trial was 07 September 2009. Additionally, the code of ethics, good medical practices and good clinical practices established by the Health General Law of the Ministry of Public Health of Republic of Cuba (Number 41, 13 July 1983 and updated in 2010) were taken into account in this research.

Pediatric patients were included in this research once their carers (parents, family or person in custody) read, agreed and signed the written Informed Consent. This written Informed Consent was signed by the parent/guardian, medical oncologist and a psychologist (as a witness). It is important to note that prior to the signing of the written Informed Consent, aims, importance and purposes of this investigation were explained to carers, as well as all requirements for the measurements. These requirements were empty bladder, 12 h of fasting and 12 h of no physical exercises before measurements.

Sample characteristics

The inclusion criteria were the free consent of carers, the children with cancer at any stage confirmed by pathological anatomy and oncological patients at the

Oncology and Hematology department in the Hospital Infantil Sur Antonio María Béguez César. The exclusion criteria were carers/patients who did not wish to participate in the research and/or children had significant alterations, such as amputees, with generalized skin diseases, serious infections, symptomatic congestive heart failure, body fluid disorders and hemostatic. The interruption criteria were voluntary abandonment and death of the cancer patient.

The sample consisted of 43 untreated cancer children, ages 2 to 17. These patients were divided into two experimental groups. The first formed by 25 patients with different histological varieties of Ts and the second consisted of 18 patients with various types of Tns. The individual analysis of each patient was performed by each age group and gender, taking into account [16]. Each patient was assigned a numerical code from 1 to 43.

Measurement procedure with the Bodystat 1500-MDD

BIA analyzer

The Bodystat 1500-MDD BIA analyzer was used to estimate R (in Ω) and X_c (in Ω) in patients with Ts and Tns. Values of $|Z|$ (in Ω) and θ (in $^\circ$) were calculated from R and X_c , using the expressions and $\theta = \text{tg}^{-1}(X_c/R)$, respectively. In this study, $|Z|$ was not reported because its values were similar to those of R and their contributions on θ were also comparable. Maximum difference between R and $|Z|$ values in cancer patients was $\leq 3 \Omega$. Additionally, maximum difference between θ values was $\leq 0.01^\circ$ when R and $|Z|$ are considered on the mathematical expression for θ . These differences had no significance in the clinical order, as in [18, 21, 22].

Although this device operated at frequencies of 5 and 50 kHz, the body values of R , X_c , $|Z|$ and θ were reported only at 50 kHz. The amplitude of the sinusoidal electric current applied was 800 μA . Additionally, the calibrator ($500.0 \pm 0.1 \Omega$) was supplied by the manufacturer of the Bodystat 1500-MDD BIA analyzer and used to assess the stability of this device at the beginning and at the end of measurement in each patient.

This study was governed by the same methodology established in [18, 21, 22] and recommendations established by the National Institutes of Health Technology Assessment Conference Statement for the measurement of bioelectrical parameters [37]. For the measurement of R_p and X_{c_p} values (the subscript p was referred to the cancer patient), the following methodology was followed [18, 21, 22]. First, H and the weight of cancer patient were measured with a medical mechanical scale with stadiometer (model ZT-120, Zheiang, China) of accuracy ± 0.1 . The minimum value of weight per division was 0.5 Kg and the minimum value height per division was 0.5 cm.

Second, patients covered with light clothing were placed in the supine position on a non-conductive surface, without

a pillow under the head, with the arms separated at approximately 30° from the thorax and the legs separated approximately at an angle of 45° without contact between them. The skin of each patient was first cleaned with water and soap, and then 70% alcohol.

Third, the stimulating electrodes (or injection electrodes of alternating electric current) were placed in the medial areas of the dorsal surfaces of hands and feet, near the metacarpal and metatarsal phalangeal joints, respectively. The sensing electrodes (or receiving electrodes the body electrical voltage) were placed between the distal epiphyses of the radius and the ulna, at the level of the pisiform eminence, as well as at the midpoint between both malleoli, respectively. The distance between the sensing and stimulating electrodes was 5 cm and measured with a standard measuring tape (Lotus model, Ningbo Sunshine Company, Ningbo, China) of 0.1 cm precision. Electrocardiogram electrodes (model APR-020, All Pro Corporation Company, Qingdao, China) were used. The material of each electrode was Silver/Silver Chloride (Ag/AgCl).

Fourth, R_p and Xc_p measurements were carried out in controlled environmental conditions of temperature (25.0 ± 1.0 °C), relative humidity (60 to 65%) and free environment of devices generating field and electromagnetic radiation. These two physical quantities were measured with a digital humidity and relative temperature meter Testo (model 608-H1, Shanghai, China). The accuracy of this instrument was ± 0.5 °C and $\pm 3\%$ for temperature and relative humidity, respectively. In addition, R_p and Xc_p measurements in each patient were between 8 and 9 am, by a previously trained nurse.

Comparison between apparently healthy and sick subjects

Average values of $(R/H)_r$, $(Xc/H)_r$ and θ_r were taken as references. This was argued because BioScan 98 and Bodystat 1500-MDD BIA analyzers were electrically equivalent, as demonstrated in [18]. The subscript r was referred to the apparently healthy subjects. This population was used as reference. The means ± 2 standard deviations of $(R/H)_r$, $(Xc/H)_r$ and θ_r of apparently healthy children by age group and gender were reported in [16]. These ranges were displayed in Table 1 to facilitate the reading of this study. Data shown in this table were provided by MSc. Alcibiades Lara Lafargue (researcher in charge of the population study in apparently healthy subjects). The latter was conducted at the Centro Nacional de Electromagnetismo Aplicado, Universidad de Oriente in Santiago de Cuba, Cuba (this institution will keep the original data of this population study for 15 years, according to the regulations established by the Ministry of Public Health of the Republic of Cuba).

The interval 17–59 was added in this study because a cancer infant was 17 years old (Table 1). $(R/H)_p$ and $(R/H)_r$, $(Xc/H)_p$ and $(Xc/H)_r$, and θ_p and θ_r were compared.

Table 1 Means ± 2 standard deviations of bioelectric parameters per height unit for apparently healthy pediatric individuals, by gender and age group

Age group (years)	Gender	$(R/H)_r$ (Ω/m)	$(Xc/H)_r$ (Ω/m)	θ_r (°)	$r(R,Xc)_r$
2–3	M,F (N = 61)	741.4 \pm 79.2	70.9 \pm 8.1	5.5 \pm 0.5	0.67
4–5	M,F (N = 91)	651.2 \pm 65.6	63.2 \pm 6.4	5.6 \pm 0.5	0.55
6–7	M,F (N = 165)	578.5 \pm 52.4	57.5 \pm 6.3	5.7 \pm 0.5	0.60
8–9	M,F (N = 179)	513.0 \pm 51.1	51.0 \pm 5.2	5.7 \pm 0.4	0.67
10–11	M,F (N = 196)	461.3 \pm 59.6	47.0 \pm 5.9	5.8 \pm 0.6	0.59
12	M,F (N = 109)	419.6 \pm 50.8	43.6 \pm 5.0	5.9 \pm 0.5	0.71
13–16	M (N = 101)	335.2 \pm 48.7	37.0 \pm 4.9	6.3 \pm 0.5	0.71
	F (N = 161)	413.0 \pm 45.8	43.6 \pm 4.7	6.1 \pm 0.5	0.69
17–59	M (N = 1263)	292.3 \pm 45.8	33.8 \pm 3.6	6.6 \pm 0.5	0.72
	F (N = 1399)	398.0 \pm 46.8	42.0 \pm 5.2	6.0 \pm 0.5	0.71

Height, male gender and female gender were represented by H, M and F, respectively. $(R/H)_r$, $(Xc/H)_r$, θ_r and $r(R,Xc)_r$ ($r(R,Xc)_r = r$) were body electrical resistance/height, body capacitive electric reactance/height, body phase angle and correlation coefficient of Pearson, respectively [16] (courtesy of MSc. Alcibiades Lara Lafargue and Centro Nacional de Electromagnetismo Aplicado)

This comparison allowed us to know if a population of pediatric patients with cancer differed from that of the apparently healthy subjects, for each age group, gender and experimental group.

Since the Xc/H versus R/H plot was a two-dimensional Euclidean space, the ordered pair $(R/H, Xc/H)$ was interpreted as the body bioelectric state of any subject from the bioelectrical point of view. In this study, body bioelectric states of the apparently healthy subject were represented by the ordered pair $((R/H)_r, (Xc/H)_r)$. Body bioelectric states of the patient with Ts/Tns were denoted by the ordered pair $((R/H)_p, (Xc/H)_p)$. Additionally, the body bioelectric state of each apparently healthy subject could be symbolized by the ordered pair (R_r, Xc_r) . The body bioelectric state of each untreated cancer pediatric patient could be represented by the ordered pair (R_p, Xc_p) . These two later asseverations were argued because the measurement was made in the same subject.

Statistical analysis

Spearman's rank correlation coefficient (or Spearman's rho) and Pearson correlation were used to know the lineal correlation between two variables: R_p and Xc_p , $(R/H)_p$ and $(Xc/H)_p$, θ_p and R_p , θ_p and Xc_p , θ_p and $(R/H)_p$, and θ_p and $(Xc/H)_p$ for the solid and non-solid tumors. Probability (p -value) was associated to each correlation analysis. Lineal correlation was significant when $p < 0.05$ (significance level).

Euclidean distance

The Euclidean distance, named d_{pr} (Ω/m), between two points $((R/H)_p, (Xc/H)_p)$ and $((R/H)_r, (Xc/H)_r)$ was calculated by means of the following equation

$$d_{pr} = \sqrt{\left[\left(\frac{R}{H}\right)_p - \left(\frac{R}{H}\right)_r\right]^2 + \left[\left(\frac{Xc}{H}\right)_p - \left(\frac{Xc}{H}\right)_r\right]^2} \tag{1}$$

In eq. (1), d_{pr} was calculated taking into account the gender, age and experimental group.

As $((R/H)_r, (Xc/H)_r)$ represented the central point of the reference rectangle and $((R/H)_p, (Xc/H)_p)$ the bioelectrical state of any cancer child for each gender and age group, their impedance vectors referred to coordinate origin (0, 0) were \vec{Z}_r and \vec{Z}_p , respectively. Consequently, \vec{Z}_r and \vec{Z}_p were position vectors. Their respective modules were $|\vec{Z}_r|$ and $|\vec{Z}_p|$. It is important to point out that d_{pr} should not be confused with $|\vec{Z}_r|$ and $|\vec{Z}_p|$. d_{pr} was the modulus of the difference between \vec{Z}_r and \vec{Z}_p , given by $d_{pr} = |\vec{Z}_p - \vec{Z}_r| = \left[|\vec{Z}_r|^2 + |\vec{Z}_p|^2 - 2|\vec{Z}_r||\vec{Z}_p|\cos(\vec{Z}_p, \vec{Z}_r)\right]^{1/2}$, where $\cos(\vec{Z}_r, \vec{Z}_p) = \frac{\vec{Z}_r \cdot \vec{Z}_p}{|\vec{Z}_r||\vec{Z}_p|}$. It should be noted that the angle between \vec{Z}_r and \vec{Z}_p did not coincide with θ_r or θ_p . It was demonstrated that $\cos(\vec{Z}_r, \vec{Z}_p) = \frac{\vec{Z}_r \cdot \vec{Z}_p}{|\vec{Z}_r||\vec{Z}_p|} = r$ [23].

From the mathematical point of view, d_{pr} denoted the ordinary distance between two points in the plane Xc/H-R/H. Nevertheless, from the bioelectric point of view, d_{pr} meant how different the body bioelectric state of a cancer child was with respect to that of a reference population, for the same age group and gender. In other words, d_{pr} was a measure of how the body bioelectric state of pediatric patient was affected by the presence of Ts/Tns. From the biophysical-chemical-energetic-clinical points of view, an increase in d_{pr} was related to a greater degradation, smaller survival and quality of life of newly diagnosed cancer children. As d_{pr} was reported for the first time in the literature, a scale for d_{pr} was suggested: 1–50; 51–100; 101–150; 151–200; 201–250; 251–300; 301–350 and > 350 Ω/m, assuming that $d_{pr} \geq 50 \Omega/m$ could have significant implications on the body bioelectric state of a cancer patient. The case of $d_{pr} = 0$ corresponded to the apparently healthy subject.

Information processing

A database (in .txt) was created for information processing. The results were presented in tables and graphs. A computer program was implemented in GNU Octave 4.0 software (free software, License 2015-05-29, Universidad de Oriente, Santiago de Cuba, Cuba) to show figures. As part of the GNU Project, GNU Octave is free software under the terms of the GNU General Public License. The website was <http://gnu.org/software/octave>.

Free Software Foundation funds the GNU Project. Developer(s): John W. Eaton and many collaborators. This software was executed in a 256-core processor HPC with 256 GB RAM.

Pearson and Spearman’s rho correlation coefficients were implemented in the statistical program Minitab 14 (Minitab Inc. for Windows, 2003, free software, National Institute of Standards and Technology, Pennsylvania State University, USA, <https://www.minitab.com/en-mx/products/minitab>). This program ran on a computer (Departamento de Matemática, Universidad de Oriente) with operating system Windows 8 con RAM 2.6 GB; 64 bits, processor 64, Inter R cor etm). The duration of the statistical processing of data was approximately 2 s.

Data will be kept for 15 years in the Oncology and Hematology department of the hospital Infantil Sur Antonio María Béguez César.

Results

Pearson and Spearman’s rho correlation coefficients gave similar results when two bioelectrical parameters of cancer patients were compared. For solid tumors, correlation coefficients (p-value) between $(R/H)_p$ and $(Xc/H)_p$, θ_p and $(R/H)_p$, and θ_p and $(Xc/H)_p$ were 0.49 ($p = 0.001$), -0.123 ($p = 0.433$) and 0.313 ($p = 0.041$), respectively. The samples used for these correlations are shown in Table 2. For non-solid tumors, correlation coefficients (p-value) between $(R/H)_p$ and $(Xc/H)_p$, θ_p and $(R/H)_p$, and θ_p and $(Xc/H)_p$ were 0.42 ($p = 0.002$), -0.134 ($p = 0.513$) and 0.298 ($p = 0.036$), respectively. The samples used for these correlations are shown in Table 3. For both tumor types, similar correlation coefficients were reported when the analysis included R_p and Xc_p , θ_p and R_p and θ_p and Xc_p .

The code, cancer histological variety, age, gender, height and values of R_p , $(R/H)_p$, Xc_p , $(Xc/H)_p$, θ_p and d_{pr} for each patient with Ts and Tns were showed in Tables 2 and 3, respectively. R_p , $(R/H)_p$, Xc_p , $(Xc/H)_p$ and θ_p were used to refer the values of R, R/H, Xc, Xc/H and θ for these patients. 58.14% (25/43) corresponded to patients with Ts and 41.86% (18/43) related to patients with Tns were revealed in these two tables. In addition, Table 2 revealed that 76.00% (19/25) of Ts were distributed among non-Hodgkin lymphoma (12/25 = 48.00%) and central nervous system (7/25 = 28.00%) tumors. 88.89% (16/18) of Tns corresponded to acute lymphoid leukemia (Table 3). Of the total number of patients, 37.21% (16/43), 27.91% (12/43) and 16.28% (7/43) corresponded to patients with acute lymphoid leukemia, non-Hodgkin lymphoma and nervous system central tumors, respectively. Of the 25 patients with Ts, 76.00% (19/25) related to the male gender and 24.00% to females. Of the 18 patients with Tns, 61.11% (11/18) corresponded to the male gender and 38.89% (7/18) to the female gender.

Table 2 Different variables for each patient with solid tumor

C	Histological variety	Age (years)	Gender	W (kg)	H (m)	R_p (Ω)	$(R/H)_p$ (Ω/m)	X_{c_p} (Ω)	$(Xc/H)_p$ (Ω/m)	θ_p ($^\circ$)	d_{pr} (Ω/m)
1	Nephroblastoma ¹	2	F	12	0.87	650	747.13	41.0	47.13	3.6	24.95
2	Testicle	2	M	11	0.88	705	801.14	51.2	58.18	4.2	61.08
3	Histiocytosis*	2	M	13	0.96	804	837.50	60.2	62.71	4.3	96.45
5	CNS	3	F	17	1.03	833	808.74	76.7	74.47	5.3	67.43
6	NHL	3	M	11	0.88	837	951.14	56.2	63.86	3.8	209.85
11	NHL	4	M	21	1.07	726	678.50	57.8	54.02	4.6	28.81
12	NHL	4	M	20	1.02	872	854.90	57.3	56.18	3.8	203.82
13	Fibrosarcoma ²	5	M	25	1.25	612	489.60	53.6	42.88	5.0	162.87
14	NHL	5	M	22	1.05	901	858.10	51.4	48.95	3.3	207.39
15	CNS	5	F	19	1.10	724	658.18	59.8	54.36	4.7	11.26
16	NHL	5	M	15	1.35	847	627.41	60.4	44.74	4.1	30.11
17	NHL	6	F	22	0.70	735	1050.00	36.3	51.86	2.8	471.53
19	CNS	7	M	24	1.20	740	616.67	60.8	50.67	4.7	38.77
20	CNS	7	F	19.5	1.19	1057	888.24	70.1	58.91	3.8	309.74
21	NHL	8	M	26	1.22	873	715.57	77.4	63.44	5.1	202.96
22	Histiocytosis*	8	M	24	1.45	732	504.83	61.1	42.14	4.8	12.06
23	NHL	10	M	25	1.26	777	616.67	56.6	44.92	4.2	155.38
25	Osteosarcoma	11	F	29	1.38	1017	736.96	71.0	51.45	4.0	275.19
26	NHL	11	M	49	1.39	611	439.57	60.3	43.38	5.6	22.03
27	NHL	11	M	40	1.50	609	406.00	60.4	40.27	5.7	55.71
30	CNS	12	M	35	1.40	642	458.57	58.3	41.64	5.2	39.02
32	NHL	12	M	49	1.45	754	520.00	65.9	45.45	5.0	100.42
37	NHL	15	M	63	1.86	511	274.73	41.6	22.37	4.7	62.21
40	CNS	15	M	48	1.60	673	420.63	49.5	30.94	4.2	85.64
43	CNS	17	M	60	1.73	580	335.26	57.7	33.35	5.7	42.96

¹Right kidney. ²Right gluteus. *Benign process with malignant behavior. Code (C), male gender (M), female gender (F), weight (W) and height (H) for each patient were specified. CNS symbolized Central Nervous System. NHL denoted Non-Hodgkin Lymphoma. R_p , $(R/H)_p$, X_{c_p} , $(Xc/H)_p$ and θ_p were the body electrical resistance, R_p per unit of height, the body capacitive electrical reactance, X_{c_p} per unit of height and the body phase angle of each patient, respectively. d_{pr} represented the distance between the points $((R/H)_r, (Xc/H)_r)$ and $((R/H)_p, (Xc/H)_p)$, for each gender and age group. The subscript p was referred to the solid tumor child while the subscript r to the population of apparently healthy children. Values of $(R/H)_r$ and $(Xc/H)_r$ were shown in Table 1 and reported in [16] (courtesy of MSc. Alcibiade Lara Lafargue and Centro Nacional de Electromagnetismo Aplicado)

Of the total number of patients, 69.77% (30/43) and 30.23% (13/43) belonged to the male and female genders, respectively.

The highest d_{pr} value of all patients with Tns and Ts was observed for Code 10 (Table 2) and Code 17 (Table 3), respectively. Of the total number of patients, 39.53% (17/43), 25.58% (11/43), 6.98% (3/43), 4.65% (2/43), 13.95% (6/43), 2.32% (1/43), 4.65% (2/43) and 2.32% (1/43) were distributed on the scale of d_{pr} 1–50, 51–100, 101–150, 151–200, 201–250, 251–300, 301–350 and > 350 Ω/m , respectively. 33.33% (9/27), 22.22% (6/27), 7.41% (2/27), 7.41% (2/27), 18.53% (5/27), 3.70% (1/27), 3.70% (1/27) and 3.70% (1/27) of the patients with Ts were distributed in the d_{pr} 1–50 scales 51–100, 101–150, 151–200, 201–250, 251–300, 301–350 and > 350 Ω/m , respectively. For these respective d_{pr} scales, distribution percentages of patients with Tns were

50.00% (8/16), 31.25% (5/16), 6.25% (1/16), 0.00% (0/16), 6.25% (1/16), 0.00% (0/16) and 6.25% (1/16).

For each gender and age group shown in Table 1, all possible combinations of $(R/H)_r$ and $(Xc/H)_r$ for a population of apparently healthy pediatric subject were included in delimited rectangles with continuous and dashed lines for the male and female genders, respectively (Fig. 1). This meant that body bioelectric-physiological states of these subjects were only possible if they belonged to the interior and contour of their respective rectangles. In other words, these states were not possible outside of them. R/H and Xc/H values outside the rectangle represented a subject with some type of pathology (for example, cancer patients), for each gender and age group. Therefore, in this study, this rectangle for apparently healthy subjects was named the reference rectangle for body bioelectric states

Table 3 Different variables for each patient with non-solid tumor

C	Type of tumor	Age (years)	Gender	W (kg)	H (m)	R_p (Ω)	$(R/H)_p$ (Ω/m)	Xc_p (Ω)	$(Xc/H)_p$ (Ω/m)	θ_p ($^\circ$)	d_{pr} (Ω/m)
4	CML	3	M	15	1.09	751	688.99	39.2	35.96	3.0	62.99
7	ALL	3	M	12	0.95	824	867.37	37.7	39.68	2.6	129.78
8	ALL	3	F	16	0.95	674	709.47	80.3	84.53	4.3	34.71
9	ALL	3	M	12	0.95	825	868.42	37.7	39.68	2.6	130.80
10	ALL	3	M	20	1.45	607	418.62	39.1	26.97	3.7	325.76
18	ALL	6	M	29	1.10	623	566.36	48.9	44.45	4.5	17.82
24	ALL	10	M	33	1.50	752	501.33	67.4	44.93	5.1	40.09
28	ALL	11	M	35	1.48	701	473.65	46.5	31.42	3.8	18.88
29	AML	12	F	35	1.52	786	517.11	51.0	33.55	3.7	98.02
31	ALL	12	M	28	1.40	889	635.00	63.1	45.01	4.4	215.41
33	ALL	12	M	29	1.76	659	374.43	50.7	28.81	4.4	47.53
34	ALL	13	F	54	1.57	755	480.89	69.9	44.46	5.3	67.90
35	ALL	13	F	57	1.64	714	435.37	58.0	35.37	4.6	23.83
36	ALL	14	F	47	1.63	833	541.72	76.7	47.06	5.3	98.10
38	ALL	15	F	92	1.70	606	356.47	55.0	32.35	5.2	57.64
39	ALL	15	F	44	1.55	683	440.65	59.9	38.65	5.0	28.09
41	ALL	15	M	82	1.87	508	271.66	45.2	24.17	5.1	64.82
42	ALL	16	M	80	1.71	512	299.42	53.5	31.29	6.0	36.24

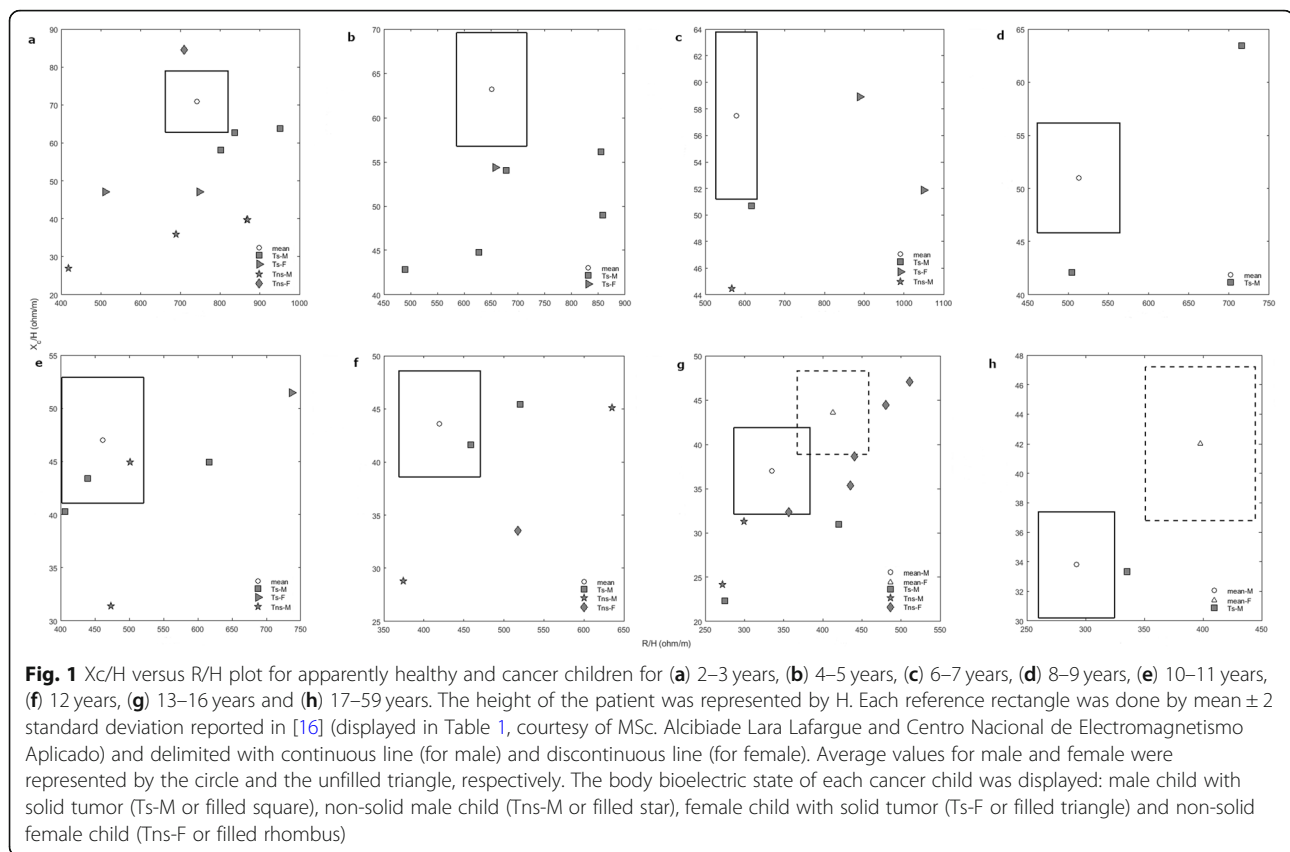
Code (C), male gender (M), female gender (F), weight (W) and height (H) for each non-solid tumor patient were specified. CML represented the chronic myeloid leukemia. ALL denoted the acute lymphoid leukemia and AML the acute myeloid leukemia. R_p , $(R/H)_p$, Xc_p , $(Xc/H)_p$ and θ_p were the body electrical resistance, R_p per unit of height, the body capacitive electrical reactance, Xc_p per unit of height and the body phase angle of each patient, respectively. d_{pr} symbolized the distance between the points $((R/H)_r, (Xc/H)_r)$ and $((R/H)_p, (Xc/H)_p)$, for each gender and age group. The subscript p was referred to the non-solid tumor child while the subscript r to the population of apparently healthy children. Values of $(R/H)_r$ and $(Xc/H)_r$ were shown in Table 1 and reported in [16] (courtesy of MSc. Alcibiade Lara Lafargue and Centro Nacional de Electromagnetismo Aplicado)

(R_r) . The normal intervals for each rectangle displayed in Fig. 1 were made using ± 2 standard deviations of reference source data [16], as displayed in Table 1.

In Fig. 1, the center circle in R_r delimited with a continuous line named (R_{rc}) represented the ordered pair $((R/H)_r, (Xc/H)_r)$ for the male gender. The unfilled triangle in the center of the R_r delimited with dashed line, named R_{rd} , symbolized the ordered pair $((R/H)_r, (Xc/H)_r)$ for the female gender. In addition, R_{rc} , R_{rd} and the body bioelectric state of each male and female patient with Ts and Tns were displayed in this figure for 2–3 years (Fig. 1a), 4–5 years (Fig. 1b), 6–7 years (Fig. 1c), 8–9 years (Fig. 1d), 10–11 years (Fig. 1e), 12 years (Fig. 1f), 13–16 years (Fig. 1g) and 17–59 years (Fig. 1h). Additionally, Fig. 1 showed that 93.02% (40/43) of pediatric patients with cancer were outside their respective R_r . Three patients (Codes 24, 26 and 30) were only in their corresponding R_r , according to the age group. Of these 40 patients, 72.5% (29/40) had $(Xc/H)_p < (Xc/H)_r$ while values of $(R/H)_p$ were distributed along the R/H axis. 90.70% (39/43) of all patients had a $\theta_p < \theta_r$, except those labeled with Codes 5, 26, 27 and 42. This condition for θ_p was observed in 88.00% (22/25) and 94.44% (17/18) of patients with Ts and Tns, respectively.

In Fig. 2, R_{rc} and R_{rd} of all apparently healthy pediatric subjects were shown. The set of these R_{rc} and R_{rd} defined the entire region in which were most likely present all bioelectric states of them. In addition, the body bioelectric state of each male and female cancer patient was illustrated in this figure in order to know if the body bioelectric state of the pediatric patient depended on gender, age group and tumor histological variety.

Figure 2 revealed that 55.81% (24/43) of body bioelectric states of cancer patients were distributed in R_{rc} or their respective neighborhoods, by gender, age group and experimental group. The body bioelectric states of the remaining patients 44.19% (19/43) were distributed regardless of gender and age group. These findings were observed in 60.00% (15/25) and 50.00% (9/18) of patients with Ts and Tns, respectively. Unlike Fig. 1, the overlapping of the body bioelectric states of patients with Tns (Codes 7 and 9, 24 and 34) and Ts (Codes 26 and 30, 13 and 22, 11 and 15) was showed in Fig. 2. Furthermore, there was an overlap of the body bioelectric states in some patients with cancer (Codes 37 and 41; 38 and 43; 13 and 34; 24 and 32; 5, 22 and 36).



Discussion

The results of this study are valid for the research period and the number of patients who fulfill the inclusion criteria. These inclusion criteria and low prevalence of cancer children in the province of Santiago de Cuba may explain why the sample size of this study is lower. In addition, the race of cancer children in this study is the same than the one reported in [16] because the ethnography of Santiago de Cuba population is characterized by a mixture of several race ethnicities (European whites, aboriginal Indians and African blacks). Nevertheless, the gender ratio of cancer children is different to that reported in [16]. This difference may be explained because gender ratio can be controlled/fixed in a population study, but not in a study with cancer patients. Gender ratio of cancer patients depends on disease prevalence for gender and age group, and inclusion, exclusion and interruption criteria.

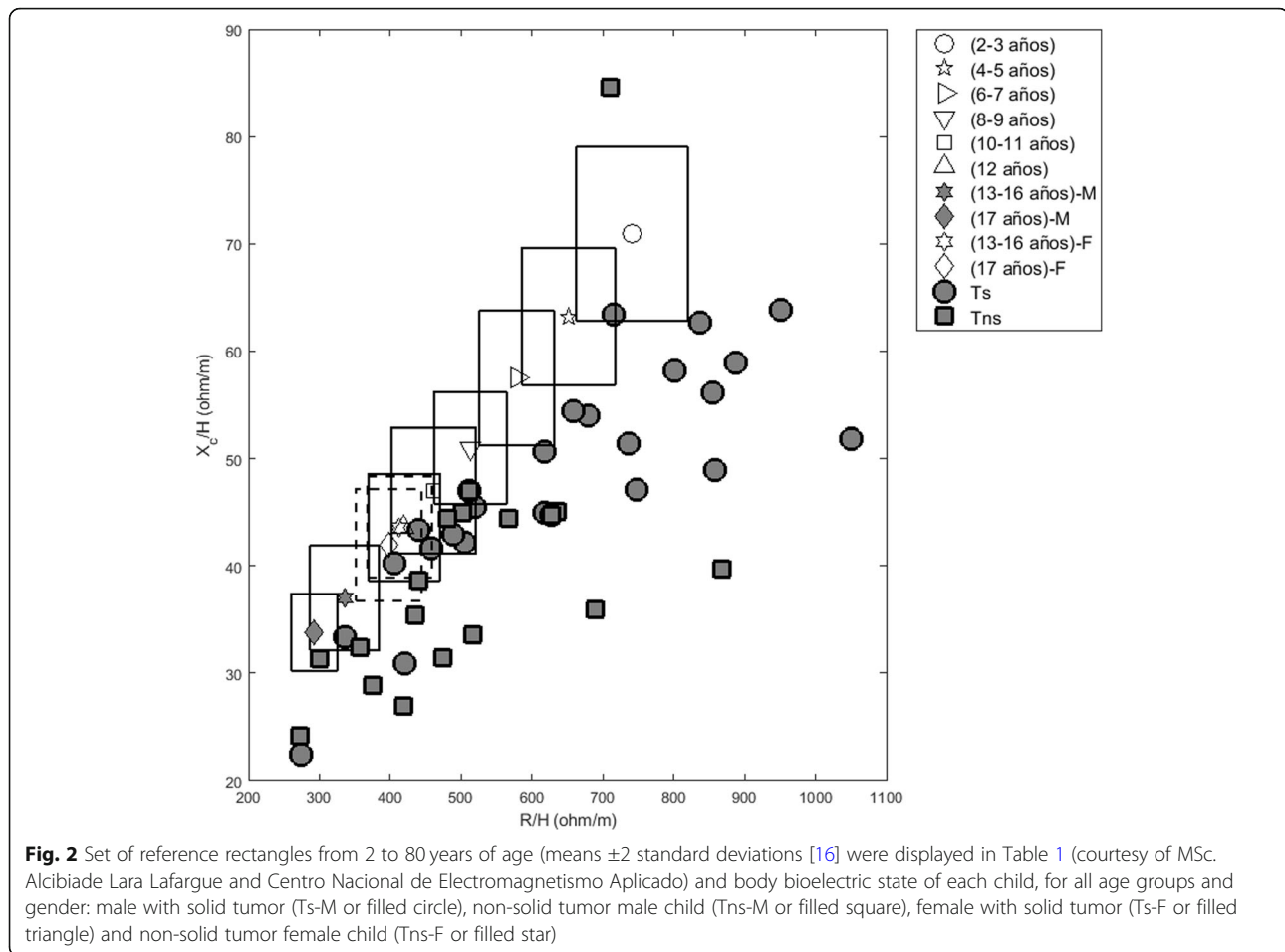
On the other hand, results of this study confirm that acute lymphoid leukemia, non-Hodgkin lymphoma and cancer of the central nervous system are most frequently observed in untreated pediatric patients, as in [2–4, 38–41]. Additionally, this study confirms that acute lymphoid leukemia is more frequent than acute myeloid leukemia, in agreement with [39, 41]. The predominance of the male gender of these patients confirms the result

documented in [42] and contradicts that reported by Toquica et al. [41].

For both tumor types, p -values indicated that correlation between θ_p and $(R/H)_p$ was non-significant and therefore non-linear. Nevertheless, significant, linear and low correlations were reported for $((R/H)_p$ and $(Xc/H)_p$) and $(\theta_p$ and $(Xc/H)_p$).

Several reasons can be attributed to nearly 10% of cancer patient not satisfying the criteria of phase angle, such as: the biological individuality, the phase angle does not have to change once the cancer patient is diagnosed for the first time, not all new diagnosed cancer children have the same performance status and detected at the same time and not all tumor type influences equally θ_p . These reasons justify why the individual analysis of the bioelectrical parameters is suggested in this study.

The finding that 90.70% of all cancer patients satisfy $\theta_p < \theta_r$ confirms that the phase angle may be used as an indicator of disease severity and quality of life and loss of body homeostasis of the cancer patient, a matter that agrees with [14]. These findings have been confirmed in adult patients with cancer [8, 42, 43] and in patients with other pathologies [8, 13, 15, 34, 44]. Gupta et al. [42] report an average survival less than 3 months in patients with lung cancer whose θ_p values are between 2 and 3°. This finding is confirmed in other studies [8, 13,



15, 34, 42–44]. Nevertheless, the effect of θ_p on the survival is not discussed in this work because no patient dies.

In this study, $\theta_p < \theta_r$ may be explained because in the majority of cancer patients prevails that $(Xc/H)_p < (Xc/H)_r$ for all value of $(R/H)_p$, for each age group, gender and experimental group. This may suggest that component $(Xc/H)_p$ of the ordered pair $((R/H)_p, (Xc/H)_p)$ prevails in the body bioelectric state of the cancer patient. From the biophysical point of view, $(Xc/H)_p$ cannot decrease until zero because θ_p tends toward zero, which means the death of the cancer patients. This occur for all values of $(R/H)_p$, confirming that $(R/H)_p$ and θ_p are not linearly correlated. This may suggest that $(Xc/H)_p$ decreases until its minimum value that brings about a quicker decrease of $(R/H)_p$ than $(Xc/H)_p$ so that θ_p stays in its normal range. From the thermodynamic point of view, a quick decrease of $(R/H)_p$ may mean the occurrence of different self-organized biophysical-chemical processes in the organism that reduce the body bioenergetics losses to guarantee its maximum survival and self-preservation as a living system. One of the main characteristics of the biological organisms, as open systems, is to tend toward its maximum survival.

If net inductive effects of the patient [45] are neglected, Xc_p may be due to the different total capacitive electrical reactance contributions of the tumor (named Xc_t), healthy tissue (Xc_o) and tumor-surrounding healthy tissue interface (named Xc_{o-t}). This interface is the tumor micro-environment and constitutes by the mixture of cancer cells, normal cells and other components. Xc_p may be expressed in a first approximation as $Xc_p \cong Xc_t + Xc_o + Xc_{o-t}$. As the capacitive contribution predominates in each tissue, $Xc = 1/(2\pi fC)$, where C is the electrical capacity of the biological tissue under consideration and f is the working frequency (50 kHz). For this reason, Xc_p , Xc_t , Xc_o and Xc_{o-t} may be substituted for their respective electrical capacities. Therefore, C_p may be calculated approximately as $C_p \cong C_t C_o C_{o-t} / (C_o C_{o-t} + C_t C_{o-t} + C_t C_o)$, where C_p , C_t , C_o and C_{o-t} are the total electrical capacities of the entire patient, the tumor, the healthy tissue and the surrounding healthy tissue-tumor interface, respectively.

It has been experimentally documented that $C_o > C_t$ (e.g., $C_t = 3.546 \pm 1.931$ pF for lung cancer and $C_o = 893 \pm 572$ pF for normal lung tissue) and the increase in capacitance of normal cells when cancer cells are added

to them [46]. The first finding is confirmed by other authors [47–50]. The second finding may mimic the mixture of cancer and normal cells in the tumor surrounding healthy tissue interface. These two findings may suggest that $C_o C_{o-t} > C_t C_o > C_t C_{o-t}$ and therefore $C_p \cong C_t$.

In addition, $C_p \cong C_t$ may also be obtained if contributions of $X_{C_{o-t}}$ to X_{C_p} (C_{o-t} to C_p) are neglected with respect to those of X_{C_t} and X_{C_o} (C_t and C_o). In this case, $(Xc)_p \cong (Xc)_t + (Xc)_o$ and $C_p \cong C_t C_o / (C_t + C_o)$. $C_p \cong C_t$ is due to the fact as normal cells have dielectric constants and membrane electrical capacities greater than those of cancer cells [46–50]. In contrast, Frike and Morse [51] report that $C_t > C_o$. The fundamental contributions of X_{C_t} and X_{C_o} to X_{C_p} may be argued because electrical activities occur mainly in the tumor and in healthy tissue (distant from the tumor). This result is expected because normal and cancerous cells are mainly confined in these two tissues and not in the tumor-surrounding healthy tissue interface. This aspect may explain in part why there are differences in the electrical properties of the tumor and healthy tissue, in agreement with others studies [47, 48, 52, 53].

The finding $C_p \cong C_t$ confirms that electrical properties and biological characteristics of the cancer histological variety significantly influence the body homeostasis, quality of life, survival and body bioelectrical and physiological parameters of a patient with Ts/Tns. Nevertheless, the tumor-surrounding healthy tissue interface cannot be completely neglected because it influences the electrical-chemical microenvironment of the tumor, which is related to the aggressiveness and metastasis of it [54–56] and its protection against the attack of cellular and humoral elements of the immune system [57, 58].

Due to the close relationship between the electrical and physiological parameters of a biological tissue [8, 21, 22, 34, 44, 58, 59], changes of C_t and X_{C_t} may be related to those of the transmembrane potential and the membrane permeability of cancer cells [47]. In turn, these changes have been related to other alterations observed in cancer cells as high mitotic activity, increase in the electronegativity of the extracellular surface, changes in intracellular and extracellular ionic concentrations, breakdown of homeostasis of electronic transport in the cell membrane, the depletion of adenosine triphosphate, the failure of the contact inhibition mechanism, morphological changes, aggressiveness, metastatic capacity, among others [47, 56, 59]. This leads to an alteration of the body homeostasis in cancer patients.

Loss of body homeostasis of a patient (child or adult) with cancer may lead to the decrease of the body cell mass and changes of its cell metabolism, body composition and distribution of total body water, as reported in [33, 60, 61]. This may explain the cachexia and modifications in $(R/H)_p$, $(Xc/H)_p$ and θ_p observed in cancer

patients, explaining in part why $(Xc/H)_p < (Xc/H)_r$ for all $(R/H)_p$ value observed in the majority of patients with Ts/Tns. This finding may suggest that losses of the body energy reserves of the patient with Ts/Tns (related to $(Xc/H)_p$) are faster than the body heat loss (related to $(R/H)_p$). This corroborates that $\theta_p < \theta_r$, as in [15, 43], and the body metabolism and body composition alterations of these cancer patients, as in [34, 60, 61]. It is important to note that heat loss is noticeable as R_p increases.

The finding $(R/H)_p > (R/H)_r$ observed in some patients with Ts/Tns may be explained because body heat loss and water and ions body imbalances in cancer patient are noticeable compared to those in apparently healthy subjects. In turn, these alterations may be related to the biophysical-chemical-bioelectrical-energetic changes in the cell membrane, as discussed above.

Despite the increase of $(R/H)_p$ in these cancer patients, θ_p decreases slightly with respect to θ_r , for each gender and age group. This may suggest that these patients still have sufficient energy reserves to compensate the possible heat loss. If these losses prevail, θ_p would decrease and therefore a low quality of life and short survival of the patient with Ts/Tns, in agreement with [42]. This statement would be noticeable when X_{C_p} also decreases, in accordance with [37].

In general, $|Z|$ and θ fix the position of any bioelectrical state in the plane R-Xc ($R/H-Xc/H$). The Cuban experience suggests that the simultaneous analysis of these two bioelectrical parameters is a necessary but not sufficient condition to absolutely differentiate one cancer patient from another or patients with any pathology from a population of apparently healthy subjects [30, 62]. This statement may be argued because cancer patients and apparently healthy individuals are inside 50 and 75% tolerance ellipses. Some of these patients evolve unfavorably during and after the application of chemotherapy. Nevertheless, other cancer patients out 95% tolerance ellipse ($3.5 < \theta_p \leq 5$) evolve favorably after this therapy [62]. Additionally, similar results are observed in lung cancer adult patients treated with surgery, radiotherapy, chemotherapy and/or immunotherapy (unpublished data). On the other hand, patients with acquired immune deficiency syndrome are also inside 50, 75 and 90% tolerance ellipses. In addition, there are no significant differences in body bioelectric parameters and body composition of these patients compared with those of an apparently healthy individual population [63].

The above-mentioned is why d_{pr} is proposed in this study. d_{pr} does not contradict $|Z|$ or θ , but they complement each other. It should be expected that there is a minimum value of d_{pr} , from which a sick subject can be differentiated from an apparently healthy subject, although the patient is in any position inside the ellipse 95% tolerance ellipse. Other distance criteria for d_{pr} may

be used, such as Mahalanobis distance [22] or a Hausdorff distance [64]. For instance, Hausdorff distance may be suggested to calculate this minimum distance. A longitudinal study is required to know this minimum value of d_{pr} .

From bivariate statistics, it is well known that tolerance ellipses can be applied if R and Xc (R/H and Xc/H) are strongly correlated ($r \geq 0.8$) [23, 31]. The values of r show in Table 1 are less than 0.8 (correlation strength between moderate and fair). Rigorously speaking, the tolerance region should not be an ellipse but a rectangle in this R-Xc (R/H-Xc/H) plot, in agreement with [23]. This and the low correlations of r^* (fair-poor) among R_p , Xc_p and θ_p ($(R/H)_p$, $(Xc/H)_p$ and θ_p) are why the rectangular tolerance region is used in this study. Rectangular tolerance region has been used in other studies [65–67]. In some studies, elliptical and rectangular tolerance regions are simultaneously analyzed [68, 69]. Additionally, the representation of multiple rectangles in the same XY plane is possible taking into account the work published by Wald [70].

As ellipse tolerance and rectangular tolerance regions (95%) are the same and the rectangle and the ellipse are both centered at the same point, an ellipse can be inscribed in a rectangle [24]. In this case, it is easy to demonstrate that the ratio of the area of the rectangle/area of the ellipse is 1.27 and the difference between their respective areas is $0.21L_1L_2$. As a result, both areas are approximately equal. L_1 ($L_1 = 2a_1$) and L_2 ($L_2 = 2a_2$) are the length and width of the rectangle, respectively. The variable a_1 is the length of the semi-major axis of the ellipse whereas a_2 is the length of the semi-minor axis. $L_1 = 2a_1$ and $L_2 = 2a_2$ guarantee the biggest area of an ellipse within a rectangle.

Unlike the studies reported in this area of knowledge, the body bioelectric state of each cancer patient is individually represented in this study. This will permit an individualized integral diagnosis and the proposal of a personalized therapy for each of them. In addition, the analysis on animals or humans is suggested individually in a previous study [71]. Therefore, each cancer patient is represented in the Xc/H versus R/H plot, according to its age and gender.

Our results suggest performing a longitudinal study that permits to know how bioelectrical and physiological parameters of these patients with Ts/Tns change over time and what relationships can be established between them. This longitudinal study will allow to establish prognostic indicators of the possible evolution of a cancer patient under the application of a therapeutic scheme.

Conclusions

In conclusion, the BIA is feasible to individualize body bioelectrical parameters and body bioelectric state in newly diagnosed cancer children and how differ from

those in apparently healthy subjects, for the same age group and gender. Additionally, the tumor electrical properties may have a noticeable role in changes of body bioelectric-physiological parameters of these newly diagnosed cancer children.

Abbreviations

BIA: Bioelectric impedance analysis; R: Body electrical resistance; Xc: Body capacitive electrical reactance; |Z|: Body electrical impedance modulus; θ : Body phase angle; H: Height of the subject; R/H: Body electrical resistance per unit of height; Xc/H: Body capacitive electrical reactance per unit of height; USA: United State of America; BIVA: Bioelectrical impedance vector analysis; r^* : Correlation coefficient of Pearson; Ts: Solid tumor; Tns: Non-solid tumor; Kg: Kilogram; cm: Centimeter; $^\circ$: Grade; %: Percentage; $(R/H)_r$: Average value of R/H for the reference population; $(R/H)_p$: Individual value of R/H for the cancer patient; $(Xc/H)_r$: Average value of Xc/H for the reference population; $(Xc/H)_p$: Individual value of Xc/H for the cancer patient; $((R/H)_r, (Xc/H)_r)$: Central point of the reference rectangle; $((R/H)_p, (Xc/H)_p)$: Bioelectrical state of any cancer child for each gender and age group; d_{pr} : Euclidean distance between two points $((R/H)_p, (Xc/H)_p)$ and $((R/H)_r, (Xc/H)_r)$; \vec{Z}_r : Position impedance vector of $((R/H)_r, (Xc/H)_r)$ referred to coordinate origin (0, 0); \vec{Z}_p : Modulus of \vec{Z}_r ; \vec{Z}_p : Position impedance vector of $((R/H)_p, (Xc/H)_p)$ referred to coordinate origin (0, 0); \vec{Z}_p : Modulus of \vec{Z}_p ; θ_r : Angle between \vec{Z}_r and x-axis (represented by R/H); θ_p : Angle between \vec{Z}_p and x-axis (represented by R/H); R_r : Reference rectangle for body bioelectric states; $R_{r,c}$: R_r delimited with a continuous line; $R_{r,d}$: R_r delimited with dashed line; Xc_p : Body capacitive electrical reactance of the patient; Xc_t : Net capacitive electrical reactance of the tumor; Xc_o : Total capacitive electrical reactance of healthy tissue (surrounding and away from the tumor); $Xc_{o,t}$: Global capacitive electrical reactance of the tumor surrounding healthy tissue interface; C: Electrical capacity of the biological tissue under consideration; f: Working frequency (50 kHz); C_p : Body electrical capacity of the patient; C_t : Net electrical capacity of the tumor; C_o : Total electrical capacity of the healthy tissue (surrounding and away from the tumor); $C_{o,t}$: Overall electrical capacity of the surrounding healthy tissue-tumor interface; L_1 : Length of the rectangle; L_2 : Width of the rectangle

Acknowledgements

We appreciate helpful questions and comments of the Editor in Chief and unknown reviewers that improve our manuscript. The authors thank the valuable help of Mario Hechevarría Sánchez, Larisa Zamora Matamoros, Juan Barrera Chacón, Yenia Infantes and nurses of the Oncology and Hematology Service of the hospital Infantil Sur Antonio María Béguez César. Additionally, we would like to thank Ing. Antonio Gómez Yépez (Grupo de Terapia Metabólica, Veracruz, México), who provided the Bodystat 1500-MDD BIA analyzer.

Authors' contributions

MMG, MVJ, TRG, SCAB, JCCR and LEBC participated in study concepts. TTBL, MMG, MVJ, TRG, SCAB, ARSC, JCCR, VGSG and LEBC designed the study. MMG, MVJ, TRG and JCCR participated in data acquisition. TTBL, MMG, ARSC and LEBC participated in quality control of data and algorithms. TTBL, MMG, MVJ, TRG, SCAB, ARSC, JCCR, VGSG and LEBC analysed and interpreted the data. TTBL, ARSC and LEBC participated in statistical analysis. TTBL, MMG, MVJ, TRG, SCAB, ARSC, JCCR, VGSG and LEBC drafted the manuscript. MMG and LEBC edited the manuscript. MMG, MVJ, TRG, SCAB, ARSC, JCCR, VGSG and LEBC revised the manuscript and supervised the entire work. The authors read, reviewed and approved the final manuscript.

Funding

This work is financially supported by the Universidad de Oriente, Santiago de Cuba, Cuba, under the grants # 7227 and 7228, Cuba. In addition, Universidad de Santo Domingo, Dominican Republic, will support the payment of this manuscript once approved. The data of this study belongs to the Universidad de Oriente. This financial support is not used in the design of this protocol, the collection, analysis and/or interpretation of data, as well as in writing of this manuscript. Authors do not received direct funding. Additionally, there is not external funding source. In addition,

Facultad de Ciencias de la Universidad Autónoma de Santo Domingo, Dominican Republic, covers the cost of this manuscript.

Availability of data and materials

Original data appear explicitly in Table 2. Nevertheless, any information and additional data available on request to the corresponding author (berguesc@yahoo.com).

Ethics approval and consent to participate

The final protocol was approved by the Ethics committee (Current Controlled trials BIACANCER12032009, 12 March 2009) and Scientific Board of the hospital Infantil Sur Antonio María Béguez César, Santiago de Cuba. Written Informed Consent is obtained from each participant before entering the trial.

Consent for publication

Not applicable.

Competing interests

The authors declare that they have no competing interests. Author Victoriano Gustavo Sierra González was employed by the company Grupo de las Industrias Biotecnológica y Farmacéuticas (BioCubaFarma, La Habana, Cuba). The remaining authors declare that the research was conducted in the absence of any commercial or financial relationships that could be construed as a potential conflict of interest.

Author details

¹Departamento de Ciencias, Escuela de Física, Universidad Autónoma de Santo Domingo (UASD), Recinto Nagua, República Dominicana. ²Técnica Regional del Ministerio de Educación, Nagua, República Dominicana. ³Departamento de Farmacia, Facultad de Ciencias Naturales y Exactas, Universidad de Oriente, 90500 Santiago de Cuba, Cuba. ⁴Servicio de Oncología y Hematología del Hospital Infantil Sur Antonio María Béguez César, 90300 Santiago de Cuba, Cuba. ⁵Dirección Municipal de Salud Pública, 90500 Santiago de Cuba, Cuba. ⁶Ensayos Clínicos del Hospital Provincial Saturnino Lora, 90500 Santiago de Cuba, Cuba. ⁷Departamento de Telecomunicaciones, Facultad de Ingeniería Telecomunicaciones, Informática y Biomédicas, Universidad de Oriente, 90400 Santiago de Cuba, Cuba. ⁸Servicio de Neumología del Hospital Clínico Quirúrgico Juan Bruno Zayas, 90600 Santiago de Cuba, Cuba. ⁹Grupo de las Industrias Biotecnológica y Farmacéuticas, Avenida Independencia, No. 8126 Esquina a Calle 100, Boyeros, La Habana, Cuba. ¹⁰Departamento de Investigaciones, Centro Nacional de Electromagnetismo Aplicado, Universidad de Oriente, Ave. Las Américas s/n, 90400 Santiago de Cuba, Cuba.

Received: 2 April 2020 Accepted: 9 June 2020

Published online: 13 June 2020

References

- Estadísticas de la Organización Mundial de la Salud. Cáncer nota descriptiva no 297; 2017. Available from: <http://www.who.int/mediacentre/factsheets/fs297/es/>.
- Salud y Asistencia Social. En Oficina Nacional de Estadística e Información (ONEI). Cuba: Edición 2017, Ministerio de Salud Pública, La Habana; 2019. Available from: <http://www.onei.cu/aec2016/19SaludPública.pdf/>.
- González Gilart G, Gainza SLS, Querol Betancourt N, Jiménez Portuondo N, Sell Lluveras M. Características clínico epidemiológicas de las leucemias en el niño. *Medisan*. 2011;15(12):1714–9 Available from: http://scielo.sld.cu/scielo.php?script=sci_arttext&pid=S1029-30192011001200005.
- Verdecia Cañizares. Cáncer pediátrico en Cuba. *Rev Cubana Pediatr*. 2017; 89(1):1–3 Available from: <http://www.medigraphic.com/pdfs/revcubped/cup-2017/cup171a.pdf>.
- Corrias A, Einaudi S, Chiorboli E, Weber G, Crino A, Andreo M, et al. Accuracy of fine needle aspiration biopsy of thyroid nodules in detecting malignancy in childhood: comparison with conventional clinical, laboratory, and imaging approaches. *J Clin Endocrinol Metab*. 2001;86(10):4644–8. <https://doi.org/10.1210/jcem.86.10.7950>.
- Hu G, Li X, He B. Imaging biological tissues with electrical conductivity contrast below 1 Sm^{-1} by means of magnetoacoustic tomography with magnetic induction. *Appl Phys Lett*. 2010;97(10):103705 Available from: <http://www.ncbi.nlm.nih.gov/pmc/articles/PMC2951991/>.
- Brantlov S, Ward LC, Jødal L, Rittig S, Lange A. Critical factors and their impact on bioelectrical impedance analysis in children: a review. *J Med Eng Technol*. 2017;41(1):22–35. <https://doi.org/10.1080/03091902.2016.1209590>.
- Piccoli A, Nescolarde LD, Rosell J. Análisis convencional y vectorial de bioimpedancia en la práctica clínica. *Nefrología*. 2002;22(3):228–38 Available from: <http://www.revistanefrologia.com/es-pdf-X0211699502014897>.
- Matias CN, Santos DA, Júdice PB, Magalhães JP, Minderico CS, Fields DA, et al. Estimation of total body water and extracellular water with bioimpedance in athletes: a need for athlete-specific prediction models. *Clin Nutr*. 2016;35(2):468–74. <https://doi.org/10.1016/j.clnu.2015.03.013>.
- Heyward VH. Practical body composition assessment for children, adults, and older adults. *Int J Sport Nutr*. 1998;8(3):285–307. <https://doi.org/10.1123/ijns.8.3.285/>.
- Jemaa HB, Mankai A, Khelifi S, Minaoui R, Ghazzi D, Zediri M, et al. Development and validation of impedance-based equations for the prediction of total body water and fat-free mass in children aged 8–11 years. *Clin Nutr*. 2019;38(1):227–33. <https://doi.org/10.1016/j.clnu.2018.01.028>.
- Bellafronte NT, Batistuti MR, dos Santos NZ, Holland H, Romão EA, Chiarello PG. Estimation of body composition and water data depends on the bioelectrical impedance device. *J Electr Bioimped*. 2018;9(1):96–105. <https://doi.org/10.2478/joeb-2018-0014>.
- Maddocks M, Kon SS, Jones SE, Canavan JL, Nolan CM, Higginson IJ, et al. Bioelectrical impedance phase angle relates to function, disease severity and prognosis in stable chronic obstructive pulmonary disease. *Clin Nutr*. 2015;34(6):1245–50 Available from: <http://www.bodystat.com/wp-content/uploads/2018/04/110-NEW-Phase-angle-and-COPD-full-paper.pdf>.
- Farias CLA, Campos DJ, Bonfin CMS, Vilela RM. Phase angle from BIA as a prognostic and nutritional status tool for children and adolescents undergoing hematopoietic stem cell transplantation. *Clin Nutr*. 2013;32(3):420–5. <https://doi.org/10.1016/j.clnu.2012.09.003>.
- Visser M, van Venrooij LMW, Wanders DCM, de Vos R, Wisselink W, van Leeuwen PAM, et al. The bioelectrical impedance phase angle as an indicator of undernutrition and adverse clinical outcome in cardiac surgical patients. *Clin Nutr*. 2012;31(6):981–6 Available from: <http://research.vumc.nl/ws/portalfiles/portal/454579/hoofdstuk+4.pdf>.
- Nescolarde L, Núñez A, Bogónez-Franco P, Lara A, Vaillant G, Morales R, et al. Reference values of the bioimpedance vector components in a Caribbean population. *e-SPEN J*. 2013;8(4):e141–4 Available from: <http://upcommons.upc.edu/bitstream/handle/2117/19969/Reference%20values%20of%20the%20bioimpedance%20vector%20components%20in%20a%20Caribbean%20population.pdf>.
- Espinosa-Cuevas MDLÁ, Hivas-Rodripuez L, González-Medina EC, Atilano-Carsi X, Miranda-Alariste P, Correa-Rotter R. Vectores de impedancia bioeléctrica Para la composición corporal en población mexicana. *Rev Invest Clin*. 2007;59(1):15–24 Available from: <http://www.medigraphic.com/pdfs/revinvcli/nn-2007/nn071c.pdf>.
- Lafargue AL, Cabrales LEB, Jarque MV, Martínez YL, Díaz YO. Parámetros bioeléctricos in vitro e in vivo, estimados con los analizadores Bodystat® 1500-MDD y BioScan® 98. *Medisan*. 2013;17(9):4054–63 Available from: http://scielo.sld.cu/scielo.php?script=sci_arttext&pid=S1029-30192013000900001.
- Genton L, Herrmann FR, Spörri A, Graf CE. Association of mortality and phase angle measured by different bioelectrical impedance analysis (BIA) devices. *Clin Nutr*. 2018;37(3):1066–9 Available from: http://boris.unibe.ch/101319/7/Genton%20ClinNutr%202017_postprint.pdf.
- Ward LC. Inter-instrument comparison of bioimpedance spectroscopic analysers. *Open Med Dev J*. 2009;1:3–10 Available from: <http://benthamopen.com/contents/pdf/TOMDJ/TOMDJ-1-3.pdf>.
- González MM, Jarque MV, González TR, Cabrales LEB, Lafargue AL, Tassé JPM. Influencia de la Resistencia eléctrica en la estimación del agua corporal total y la masa libre de grasa. *Medisan*. 2013;17(10):7001–10 Available from: <http://www.medigraphic.com/pdfs/medisan/mds-2013/mds13101.pdf>.
- Cabrales IB, González MM, Cabrales LEB, Jarque MV, Tassé JPM. Validez de las ecuaciones de estimación Para la masa libre de grasa por el método de la impedancia bioeléctrica en cualquier población. *Medisan*. 2016;20(12):6055–62 Available from: http://scielo.sld.cu/scielo.php?script=sci_arttext&pid=S1029-30192016001200008.
- Rencher AC. *Methods of multivariate analysis*. 2nd ed. New York: Wiley Interscience, A John Wiley & Sons. Inc. Publication; 2002. p. 43–155. Available from: http://www.umpalangkaraya.ac.id/perpustakaan/digilib/files/disk1/18/123-dfadf-alvincrenc-870-1-method_o-s.pdf.

24. Wang FK, Hubele NF, Lawrence FP, Miskulin JD, Shahriari H. Comparison of three multivariate process capability indices. *J Qual Technol.* 2000;32(3):263–75 Available from: http://www.researchgate.net/profile/Fu_Kwun_Wang/publication/279972249_Comparison_of_Three_Multivariate_Process_Capability_Indices/links/55cd51e108aebd6b88e05fde/Comparison-of-Three-Multivariate-Process-Capability-Indices.pdf.
25. Rau GJ, Fassuliotis G. Equal-frequency tolerance ellipses for population studies of *Belonolaimus longicaudatus*. *J Nematol.* 1970;2(1):84 Available from: <http://www.ncbi.nlm.nih.gov/pmc/articles/PMC2618713/pdf/84.pdf>.
26. Piccoli A, Rossi B, Pillon L, Bucciante G. A new method for monitoring body fluid variation by bioimpedance analysis: the RXc graph. *Kidney Int.* 1994; 46(2):534–9 Available from: <http://core.ac.uk/download/pdf/82530248.pdf>.
27. Piccoli A, Nigrelli S, Caberlotto A, Bottazzo S, Rossi B, Pillon L, et al. Bivariate normal values of the bioelectrical impedance vector in adult and elderly populations. *Am J Clin Nutr.* 1995;61(2):269–70 Available from: http://s3.amazonaws.com/academia.edu.documents/42442276/Piccoli_A_Nigrelli_S_Caberlotto_A_et_al.pdf?X-Amz-Algorithm=AWS4-HMAC-SHA256&X-Amz-Credential=AKIAIWOWYYGZ2Y53UL3A%2F20200318%2Fus-east-1%2Faws4_request&X-Amz-Date=20200318T143125Z&X-Amz-Expires=3600&X-Amz-SignedHeaders=host&X-Amz-Signature=e034ff12d400da55a7255fb208ea5115fcf21236063c60dea0d889168ee80ef9.
28. Piccoli A, Pittoni G, Facco E, Favaro E, Pillon L. Relationship between central venous pressure and bioimpedance vector analysis in critically ill patients. *Crit Care Med.* 2000;28(1):132–7 Available from: http://www.mikropolis.pl/_pdf/biva_venouspresspccl.pdf.
29. Castizo-Olier J, Carrasco-Marginet M, Roy A, Chaverri D, Iglesias X, Pérez-Chirinos C, et al. Bioelectrical impedance vector analysis (BIVA) and body mass changes in an ultra-endurance triathlon event. *J Sports Sci Med.* 2018; 17(4):571 Available from: <http://www.ncbi.nlm.nih.gov/pmc/articles/PMC6243631/>.
30. Lafargue AL. Introduction of inductive elements in the Cole-Fricke-Cole model to describe the behavior of low frequency bioelectric parameters: experimental data and simulations Master thesis. Universidad de Oriente, Centro Nacional de Electromagnetismo Aplicado, Santiago de Cuba, Cuba; 2005.
31. Akoglu H. User's guide to correlation coefficients. *Turk J Emerg Med.* 2018; 18:91–3. <https://doi.org/10.1016/j.tjem.2018.08.001>.
32. Shime N, Ashida H, Chihara E, Kageyama K, Katoh Y, Yamagishi M, et al. Bioelectrical impedance analysis for assessment of severity of illness in pediatric patients after heart surgery. *Crit Care Med.* 2002;30(3):518–20. <https://doi.org/10.1097/00003246-200203000-00004>.
33. Brinksma A, Roodbol PF, Sulkers E, Kamps WA, de Bont ES, Boot AM, et al. Changes in nutritional status in childhood cancer patients: a prospective cohort study. *Clin Nutr.* 2015;34(1):66–73. <https://doi.org/10.1016/j.clnu.2014.01.013>.
34. Kyle UG, Earthman CP, Pichard C, Coss-Bu JA. Body composition during growth in children: limitations and perspectives of bioelectrical impedance analysis. *Eur J Clin Nutr.* 2015;69(12):1298. <https://doi.org/10.1038/ejcn.2015.8>.
35. Azevedo ZMA, Moore DCBC, de Matos FAA, Fonseca VM, Peixoto MVM, Gaspar-Elzas MIC, et al. Bioelectrical impedance parameters in critically ill children: importance of reactance and resistance. *Clin Nutr.* 2013;32(5):824–9. <https://doi.org/10.1016/j.clnu.2013.01.011>.
36. Williams JR. The declaration of Helsinki and public health. *Bull World Health Organ.* 2008;86(8):650–2 Available from: <http://www.ncbi.nlm.nih.gov/pmc/articles/PMC2649471/>.
37. NIH Consensus statement. Bioelectrical impedance analysis in body composition measurement. NIH Technol Assess Statement. 1994:1–35 December 12–14. Available from: <http://ci.nii.ac.jp/naid/10007076316/>.
38. Steliarova-Foucher E, Colombet M, Ries LA, Moreno F, Dolya A, Bray F, et al. International incidence of childhood cancer, 2001–10: a population-based registry study. *Lancet Oncol.* 2017;18(6):719–31. [https://doi.org/10.1016/S1470-2045\(17\)30186-9](https://doi.org/10.1016/S1470-2045(17)30186-9).
39. Gupta S, Howard SC, Hunger SP, Antillon FG, Metzger ML, Israels T, et al. Treating childhood cancer in low-and middle-income countries. In: Jamison DT, Nugent R, Gelband H, Horton S, Jha P, Laxminarayan R, editors. Disease control priorities. 3rd ed. Washington: Editorial International Bank for Reconstruction and Development, World Bank Group; 2015. p. 121–46. Available from: http://www.ncbi.nlm.nih.gov/books/NBK343628/pdf/Bookshelf_NBK343628.pdf.
40. Bravo LE, García LS, Collazos P, Aristizabal P, Ramirez O. Descriptive epidemiology of childhood cancer in Cali: Colombia 1977–2011. *Colo Med.* 2013;44(3):155 Available from: <http://www.ncbi.nlm.nih.gov/pmc/articles/PMC4002030/>.
41. Toquica CDPV, Silva PAM, Acero H. Caracterización clínico-epidemiológica de los pacientes pediátricos con leucemias agudas en la Clínica Universitaria Colombia. Serie de casos 2011–2014. *Pediatría.* 2016;49(1):17–22. <https://doi.org/10.1016/j.rcpe.2016.01.002>.
42. Gupta D, Lammersfeld CA, Vashi PG, King J, Dahlk SL, Grutsch JF, et al. Bioelectrical impedance phase angle in clinical practice: implications for prognosis in stage IIIB and IV non-small cell lung cancer. *BMC Cancer.* 2009; 9(1):37. <https://doi.org/10.1186/1471-2407-9-37>.
43. Hui D, Bansal S, Morgado M, Dev R, Chisholm G, Bruera E. Phase angle for prognostication of survival in patients with advanced cancer: preliminary findings. *Cancer.* 2014;120(14):2207–14. <https://doi.org/10.1002/cncr.28624>.
44. Lukaski HC, Kyle UG, Kondrup J. Assessment of adult malnutrition and prognosis with bioelectrical impedance analysis: phase angle and impedance ratio. *Curr Opin Clin Nutr Metab Care.* 2017;20:330–9. <https://doi.org/10.1097/MCO.0000000000000387>.
45. Lafargue AL, Cabrales LB, Larramendi RM. Bioelectrical parameters of the whole human body obtained through bioelectrical impedance analysis. *Bioelectromagnetics.* 2002;23(6):450–4. <https://doi.org/10.1002/bem.10034>.
46. Kimura S, Morimoto T, Uyama T, Monden Y, Nouchi Y, Iritani T. Application of electrical impedance analysis for diagnosis of a pulmonary mass. *Chest.* 1994;105(6):1679–82. <https://doi.org/10.1378/chest.105.6.1679>.
47. Al Ahmad M, Al Natour Z, Mustafa F, Rizvi TA. Electrical characterization of normal and cancer cells. *IEEE Access.* 2018;6:25979–86. <https://doi.org/10.1109/ACCESS.2018.2830883>.
48. Zhang F, Jin T, Hu Q, He P. Distinguishing skin cancer cells and normal cells using electrical impedance spectroscopy. *J Electroanal Chem.* 2018;823:531–6. <https://doi.org/10.1016/j.jelechem.2018.06.021>.
49. Ermolina I, Polevaya Y, Feldman Y, Ginzburg BZ, Schlesinger M. Study of normal and malignant white blood cells by time domain dielectric spectroscopy. *IEEE T Dielect El In.* 2001;8(2):253–61. <https://doi.org/10.1109/94.919948>.
50. Qiao G, Duan W, Chatwin C, Sinclair A, Wang W. Electrical properties of breast cancer cells from impedance measurement of cell suspensions. *J Phys Conf Ser.* 2010;224:012081. <https://doi.org/10.1088/1742-6596/224/1/012081>.
51. Fricke H, Morse S. The electric capacity of tumors of the breast. *J Cancer Res Ther.* 1926;10(3):340–76. <https://doi.org/10.1158/jcr.1926.340>.
52. Bera TK. Bioelectrical impedance and the frequency dependent current conduction through biological tissues: a short review. *IOP Conf Ser: Mater Sci Eng.* 2018;331(1):012005. <https://doi.org/10.1088/1757-899X/331/1/012005>.
53. Haemmerich D, Schutt DJ, Wright AS, Webster JG, Mahvi DM. Electrical conductivity measurement of excised human metastatic liver tumours before and after thermal ablation. *Physiol Meas.* 2009;30(5):459. <https://doi.org/10.1088/0967-3334/30/5/003>.
54. Huang YJ, Hoffmann G, Wheeler B, Schiapparelli P, Quinones-Hinojosa A, Searson P. Cellular microenvironment modulates the galvanotaxis of brain tumor initiating cells. *Sci Rep.* 2016;6:21583. <https://doi.org/10.1038/srep21583>.
55. Rianna C, Radmacher M. Influence of microenvironment topography and stiffness on the mechanics and motility of normal and cancer renal cells. *Nanoscale.* 2017;9(31):11222–30. <https://doi.org/10.1039/C7NR02940C>.
56. Hanahan D, Weinberg RA. Hallmarks of cancer: the next generation. *Cell.* 2011;144(5):646–74. <https://doi.org/10.1016/j.cell.2011.02.013>.
57. Haltiwanger S. The electrical properties of cancer cells; 2008. <http://www.royallife.com/haltiwanger1.pdf> (2008).
58. Lukaski HC. Requirements for clinical use of bioelectrical impedance analysis (BIA). *Ann N Y Acad Sci.* 1999;873:72–6. <https://doi.org/10.1111/j.1749-6632.1999.tb09451.x>.
59. Diouf A, Diongue O, Nde M, Idohou-Dossou N, Thiam M, Wade S. Validity of bioelectrical impedance analysis in predicting total body water and adiposity among Senegalese school-aged children. *PLoS One.* 2018;13(10): e0204486 Available from: <http://www.ncbi.nlm.nih.gov/pmc/articles/PMC6181292/>.
60. De Santis MC, Porporato PE, Martini M, Morandi A. Signaling pathways regulating redox balance in cancer metabolism. *Front Oncol.* 2018;8:126. <https://doi.org/10.3389/fonc.2018.00126>.

61. Long J, Zhang CJ, Zhu N, Du K, Yin YF, Tan X, et al. Lipid metabolism and carcinogenesis, cancer development. *Am J Cancer Res.* 2018;8(5):778 Available from: <http://www.ncbi.nlm.nih.gov/pmc/articles/PMC5992506/>.
62. de la Cruz-López AL. Bioelectric parameters measured in cancer children treated with chemotherapy: phase diagrams Diploma thesis. Universidad de Oriente, Facultad de Ingeniería Eléctrica, Departamento Ingeniería Biomédica, Santiago de Cuba, Cuba; 2012.
63. Montoya ACR, Bourón AIN, Lafargue AL, Larramendi RM, Saní VP, Suárez GV, et al. Comparación bioeléctrica y de composición corporal en portadores y casos SIDA. *Medisan.* 2007;11(3):1–5 Available from: <http://www.redalyc.org/pdf/3684/368444988009.pdf>.
64. Elber G, Grandine T. Hausdorff and minimal distances between parametric free forms in \mathfrak{R}^2 and \mathfrak{R}^3 . In: International conference on geometric modeling and processing. Berlin: Heidelberg, Springer; 2008. p. 191–204.
65. Filzmoser P, Hron K, Reimann C. The bivariate statistical analysis of environmental (compositional) data. *Sci Total Environ.* 2010;408(19):4230–8. <https://doi.org/10.1016/j.scitotenv.2010.05.011>.
66. Chen H. A multivariate process capability index over a rectangular solid tolerance zone. *Stat Sin.* 1994;4:749–58 Available from: <http://www3.stat.sinica.edu.tw/statistica/oldpdf/a4n223.pdf>.
67. Genz A. Numerical computation of rectangular bivariate and trivariate normal and t probabilities. *Stat Comput.* 2004;14(3):251–60. <https://doi.org/10.1023/B:STCO.0000035304.20635.31>.
68. Di Bucchianico A, Einmahl JH, Mushkudiani NA. Smallest nonparametric tolerance regions. *Ann Stat.* 2001;1320–43 Available from: https://projecteuclid.org/download/pdf_1/euclid.aos/1013203456.
69. Shahriari H, Abdollahzadeh M. A new multivariate process capability vector. *Qual Eng.* 2009;21(3):290–9. <https://doi.org/10.1080/08982110902873605>.
70. Wald A. An extension of Wilks' method for setting tolerance limits. *Ann Math Stat.* 1943;14(1):45–55 Available from: https://projecteuclid.org/download/pdf_1/euclid.aoms/1177731491.
71. González MM, Morales DF, Cabrales LEB, Pérez DJ, Montijano JJ, Castañeda ARS, et al. Dose-response study for the highly aggressive and metastatic primary F3ll mammary carcinoma under direct current. *Bioelectromagnetics.* 2018;39(6):460–75. <https://doi.org/10.1002/bem.22132>.

Publisher's Note

Springer Nature remains neutral with regard to jurisdictional claims in published maps and institutional affiliations.

Ready to submit your research? Choose BMC and benefit from:

- fast, convenient online submission
- thorough peer review by experienced researchers in your field
- rapid publication on acceptance
- support for research data, including large and complex data types
- gold Open Access which fosters wider collaboration and increased citations
- maximum visibility for your research: over 100M website views per year

At BMC, research is always in progress.

Learn more biomedcentral.com/submissions

